Analytica Chimica Acta 1127 (2020) 106–113

Contents lists available at ScienceDirect

Analytica Chimica Acta

journal homepage: www.elsevier.com/locate/aca

"Signal-on" SERS sensing platform for highly sensitive and selective Pb^{2+} detection based on catalytic hairpin assembly

Yan Wu *, Cuicui Fu , Jie Xiang , Yulian Cao , Yu Deng , Rui Xu , Huan Zhang , Wenbing Shi

Chongqing Key Laboratory of Inorganic Special Functional Materials, College of Chemistry and Chemical Engineering, Yangtze Normal University, Fuling, Chongqing, 408100, China

HIGHLIGHTS

- A novel "signal-on" SERS sensing platform for Pb^{2+} was developed based on CHA amplification and DNAzymes.
- A good linear detection range for Pb^{2+} in a range from 1 pM to 100 nM with the detection limit at 0.42 pM.
- The proposed strategy can be employed for Pb^{2+} detection in real environment sample.

GRAPHICAL ABSTRACT

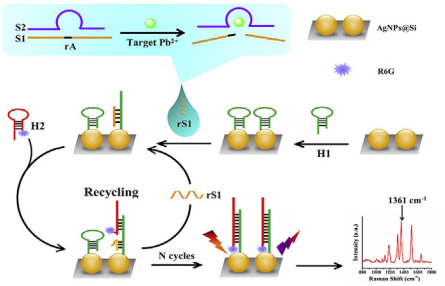

ARTICLE INFO

Article history:
Received 8 February 2020
Received in revised form
26 May 2020
Accepted 16 June 2020
Available online 8 July 2020

Keywords:
Lead ion detection
Catalytic hairpin assembly
DNAzyme
Surface-enhanced Raman scattering

ABSTRACT

In this work, a surface-enhanced Raman scattering (SERS) sensing strategy was proposed for the analysis of lead ion (Pb^{2+}) with high sensitivity and specificity based on the high specificity of the catalytic nucleic acids (DNAzymes) to Pb^{2+} and the catalytic hairpin assembly (CHA) amplification. First, the Pb^{2+}-DNAzyme initiated the reaction by target Pb^{2+} and released a linear DNA (rS1). Second, the hairpin DNA 1 (H1) was immobilized on the SERS substrate surface via Ag–S bond. Then, the rS1 could cyclically trigger the allosteric effects of CHA amplification and the H1 was opened and then the R6G-labeled hairpin probe 2 (H2) hybridized with H1 to form H1–H2 double-stranded and the released rS1 could initiate the next cycle of CHA reaction. This process made the Raman tag of R6G close to the surface of SERS substrate, and the intensity of SERS signal from R6G labels increase with the increase of concentration of target Pb^{2+}. Benefiting from outstanding performances of the Pb^{2+}-specific DNAzymes and enzyme-free CHA amplification system, this biosensor exhibits good sensitivity for Pb^{2+} with a limit of detection of 0.42 pM. More importantly, this developed detection platform could be employed for reliable analysis of Pb^{2+} in real environment system.

1. Introduction

Lead ion (Pb^{2+}) can lead to serious environment pollutant and be harmful to human health even at low concentration as one of the most toxic heavy-metal ions [1]. A very small amount of Pb^{2+} can lead to serious harm to the central nervous system and brain [2]. Considering the high toxicity of Pb^{2+}, the United States Environmental Protection Agency (EPA) has set a safety threshold level of Pb^{2+} amount in drinking water to be 483 nM (100 ppb) in blood and 72.4 nM (15 ppb) respectively [3,4]. Hence, it is considerable important to propose strategy for sensitive and specific

* Corresponding author.
E-mail address: wyan2018@163.com (Y. Wu).

https://doi.org/10.1016/j.aca.2020.06.038
0003-2670/

determination of Pb^{2+} in environment samples. Therefore, various traditional techniques have been developed for Pb^{2+} analysis, including atomic absorption spectroscopy (AAS) [5], inductively coupled plasma atomic emission spectroscopy (ICP-AES) [6], X-ray fluorescence spectroscopy [7], and inductively coupled plasma mass spectroscopy (ICP-MS) [8] etc. Although those strategies are reliable for Pb^{2+} analysis with high sensitivity, most of them still have many disadvantages, including tedious sample preparation, requiring specialized instruments and skilled operators, making them unsuitable for on-site and real-time analysis. Hence, many excellent sensors for the determination of Pb^{2+} have attracted much attention with high sensitivity, portability, low cost, minimal equipment requirements, and short response time in the past decades [9–25]. Most of them are mainly dependent on the catalytic nucleic acids (DNAzymes), which can be obtained by *in vivo* selection and specifically for Pb^{2+} [26], making the change of detection signals, such as colorimetric [9–12], electrochemical [13–16], fluorescent signals [17–20], and so forth (see Table S2). Benefiting from the high specificity of DNAzymes, these DNAzyme-based sensors exhibit good specificity for Pb^{2+}. However, it is pitiful that most of them are limited by the poor sensitivity. Therefore, exploring more sensitive sensing strategies for the analysis of Pb^{2+} is very desirable.

Recently, surface-enhanced Raman spectroscopy (SERS) sensing strategies, considered as a significant analytical platform [27–29], have been employed for the sensitive and reliable determination of Pb^{2+}, mainly benefiting from their three advantages: (1) ultrahigh sensitivity with single-molecule level limit of detection, (2) specific molecular fingerprint resulting in overcoming interference-related issues, and (3) short acquisition time and nondestructive measurement [21,22,30,31]. Although these SERS sensing strategies are excellent, the sensitivity still needs to be improved, thus limiting their practical application in the determination of Pb^{2+} [21,31]. Hence, it is imperative to develop SERS sensing strategy for ultrasensitive Pb^{2+} detection in real environmental samples.

Many amplification methods have been proposed to further enhance the sensitivity of Pb^{2+} determination, such as rolling circle amplification (RCA) [14,32], hybridization chain reaction (HCR) [33–35], and strand displacement amplification (SDA) [36] etc. Although the sensitivity of these signal amplification strategies can be significantly improved, they still have some limitations including poor reproducibility, susceptible to reaction conditions, expensive reagents, and complicated operation process. Very recently, catalytic hairpin assembly (CHA) amplification was emerged as a highly promising signal amplification strategy with enzyme-free and simple isothermal DNA reaction. Furthermore, CHA amplification could obtain hundreds-fold catalytic amplification and surmounted the limitation of traditional enzymatic amplification, for example, complicated operation, special experimental conditions, and the enzyme activity-dependent reaction time [37–42]. As a result, various CHA amplification-based sensing strategies have been proposed to determinate many targets, including electrochemical [43–45], fluorescent [46,47], colorimetric [48,49], and surface plasmon resonance methods [50,51]. These CHA amplification-based sensors exhibited excellent analytical performance with high sensitivity and specificity.

Inspired by these previous researches, a “signal-on” SERS platform based on CHA amplification and Pb^{2+}-specific DNAzymes as recognition element was proposed for highly sensitive and specific Pb^{2+} analysis for the first time in this work. The Ag nanoparticles-decorated silicon wafer was prepared as SERS-active substrate, with immobilization hairpin probe 1 (H1) on the surface via Ag–S bonds. In the presence of target Pb^{2+}, the substrate strand (S1) was specifically cleaved by Pb^{2+} and one of the two fragments (rS1) being introduced on the SERS substrate surface was hybridized with H1. The CHA amplification could be initiated to form the H1-rS1 intermediate, and then catalyzed the assembly of H1 and H2 to obtain R6G-labeled H1–H2 duplex structures following with the release of rS1. The released rS1 could further initiate the next cycle to promote the CHA recycling assembly and obtain multiple CHA products, which remarkably reduced the distance between R6G Raman labels and the surface of SERS substrate, producing strong R6G SERS signal. Therefore, the Raman intensity from R6G label increased with the increase of the concentration of target Pb^{2+}, allowing sensitive and specific determination of different concentrations of target Pb^{2+}. Benefiting from the advantages of CHA signal amplification and Pb^{2+}-specific DNAzyme, a robust SERS sensing platform was proposed for Pb^{2+} determination with high sensitivity and specificity. There are two main advantages for the developed SERS platform combined with Pb^{2+}-DNAzyme assistant CHA amplification. First, the DNAzyme as the specific recognition element for Pb^{2+} shows robust selectivity. Second, a doubly amplified strategy employing CHA amplification and DNAzyme can increase signal gain and amplification efficiency, which greatly improves the sensitivity. Comparing to the robust single-particle detection (SPD) strategy [52–54], the developed SERS sensing strategy exhibits a comparable sensitivity and selectivity. Moreover, this method was employed to determinate Pb^{2+} in real water samples and then shown excellent performance for Pb^{2+} analysis, showing a significant potential for applications in real environment analysis.

2. Materials and methods

2.1. Chemicals and reagents

All DNA oligonucleotides were synthesized by Takara Biotechnology Co. Ltd., and these sequences were shown in Table S1. 4-mercaptobenzoic acid (4-MBA) was obtained from Tokyo Chemical Industry Co., Ltd. Hydrogen peroxide, sulfuric acid, $AgNO_3$, hydrofluoric acid, tris-(2-carboxyethyl) phosphine hydrochloride (TCEP), $Pb(Ac)_2$, $MnCl_2$, $FeCl_2$, $Cd(ClO_4)_2$, $HgCl_2$, $NiCl_2$, $BaCl_2$, $CaCl_2$, $CoCl_2$, $CuCl_2$, and $ZnCl_2$ were obtained from Sinopharm Chemical Reagent Co., Ltd. All these reagents were used directly. Phosphate-doped (p-type) silicon wafers (0.01–0.05 Ω sensitivity) were obtained from Hefei Kejing Material Technology Co., Ltd. The buffers involved in this experiment are as follows: the hybridization buffer for DNA hybridization reaction was 10 mM Tris-HCl (pH 7.4) (100 mM NaCl, 1 mM EDTA, and 50 mM $MgCl_2$), HEPES buffer (50 mM HEPES (pH 7.4), 50 mM NaCl, and 5 mM $MgCl_2$), and 5 × TBE buffer (pH 8.0) (225 mM Tris-Boric acid and 50 mM EDTA).

2.2. Instruments

SERS spectra were collected by the EZRaman-M portable Raman spectrometer using a He–Ne laser (λ = 785 nm) (Enwave Optronics, Inc.). The laser power was 25 mW. The obtained spectra were further handled with the Auto Base Line of EZRaman-M Raman software. The as-prepared SERS substrate was characterized by an atomic force microscopy (AFM) (NaNoManVs) and a scanning electron microscopy (SEM) (Zeiss GeminiSEM 300). The gel electrophoresis was carried out by an electrophoresis apparatus (Tanon EPS 300, China) and imaged on a gel imaging analysis system (Tanon 1600, China).

2.3. Preparation of SERS substrate

The Ag nanoparticles-decorated silicon wafer (AgNPs@Si) was used as SERS substrate and it was fabricated via the reported method [55], which the AgNPs was *in-situ* grew on a silicon wafer.

First, the silicon wafer was further immersed into 5% HF solution for 20 min to gain H-terminated silicon wafer covered with Si–H bonds. Subsequently, the modified substrate was immediately submerged into $AgNO_3$ solution containing 10% HF for 3 min, making AgNPs grow on the silicon wafer surface via reduction reaction and obtain AgNPs@Si chip. Then the obtained chip was washed with ultrapure water for three times.

2.4. Functionalization of SERS substrate

First, the thiolated-H1 was mixed with 10 mM Tris (pH 7.4) containing 5.0 mM TCEP for 1 h. The as-prepared AgNPs@Si SERS substrate was soaked in the DNA assembly buffer containing 1.0 μM H1 probe for 24 h to conjugate the H1 probe to the surface of AgNPs. Then, the SERS substrate was treated with phosphate buffer including 0.1 M NaCl for 16 h to obtain sufficient self-assembly between AgNPs and thiolated-H1. Subsequently, the treated chip was fully washed with 100 mM PBS buffer to detach excess DNA. Second, the substrate strand S1 (1.0 μM) and enzyme strand S2 (1.0 μM) were mixed and heated to 95 °C and remained for 5 min to form Pb^{2+}-specific DNAzymes, then target Pb^{2+} solution containing different concentration of Pb^{2+} was put into the cooled mixture solution and reacted with 30 min at 37 °C. The cleavage reaction between Pb^{2+} and DNAzymes was finished. Third, 15 μL of mixture solution (containing rS1) was introduced onto the AgNPs@Si chip surface for 1 h. Last, 1.0 μM H2 probe was incubated with the chip for 60 min, the H2 induced by the strand displacement CHA amplification was completed.

2.5. SERS measurements of target Pb^{2+}

SERS measurement was conducted on an EZRaman-M portable Raman spectrometer using a He–Ne laser ($\lambda = 785$ nm) at room temperature, employing 1 s acquisition time with 3 rounds of accumulation. All Raman spectra in this work were calibrated by the EZRaman-M Raman software with Auto Base Line. Each sample measurement was performed at least for three times. Other several metal ions were also measured as the same experimental conditions as target Pb^{2+} detection.

2.6. Gel electrophoresis analysis

To testify the feasibility of CHA signal amplification, the sequences of DNA and products of the CHA amplification were evaluated by 5% agarose gel for 20 min.

3. Results and discussion

3.1. Principle of SERS sensor

When compared to free Au/Ag nanoparticles-based SERS substrates, silicon-based SERS substrates including silicon nanowire arrays, or metallic nanoparticle-decorated silicon wafers, simultaneously feature strong SERS enhancement, good uniformity, adaptable reproducibility, and superior sensitivity [56]. As a result, the AgNPs@Si was prepared as SERS substrate for constructing the SERS sensing platform. The principle of the CHA amplification-based SERS sensing strategy for Pb^{2+} analysis is illustrated in Scheme 1. First, the SERS substrate is prepared by a reported HF-etching strategy [57]: the AgNPs were immobilized on the silicon wafer surface. Afterward, the thiolated-H1 probe is linked on the AgNPs surface via Ag–S bond, which is called SERS chip. Second, the substrate strand (S1) is specifically cleaved by Pb^{2+} in the presence of target Pb^{2+}, leading to releasing of one of the two fragments (rS1). Subsequently, the rS1 is introduced into the surface of SERS chip and then hybridizes with H1 probe to active the CHA amplification and forms H1-rS1 immediate. The H1-rS1 immediate is unstable and the exposed sequence of H1 hybridizes with R6G-labeled H2 probe to form H1–H2 duplexes and the rS1 is released. More importantly, the liberated rS1 is available for the next amplification circulation and can unfold another H1 probe to initiate the assembly of H1 and H2 via CHA reaction which results in forming many H1–H2 complexes, making the Raman label R6G close to the surface of SERS substrate and the feature Raman signals of R6G (Raman peaks at 1361 cm^{-1} and 1509 cm^{-1}) generate, thus the SERS intensity of R6G is strongly enhanced induced by the silicon-assisted plasmon resonance and the Ag NP plasmon resonance. As a result, the SERS intensity of R6G continually increases with the increase of target Pb^{2+} concentration. As we all known, this is first report of “signal-on” SERS sensing platform based on CHA amplification for the detection of Pb^{2+}.

3.2. Characterization of the AgNPs@Si chip

The feature of the AgNPs@Si SERS substrate was characterized by SEM and AFM. As illustrated in Fig. 1A and B, the AgNPs are distributed uniformly on the silicon wafer surface and the AgNPs size is evaluated to be ~90 nm (inset in Fig. 1B), which is achieved by the random measurement of 300 AgNPs in the SEM image. In addition, it concludes that the AgNPs@Si SERS substrate contains Si and Ag element, which is identified by the EDX spectroscopy (Fig. 1C). The Ag peak is assigned to the element from AgNPs while the Si peak originates from the silicon wafer. The result of EDX spectroscopy indicates that the AgNPs@Si chip includes Si and Ag with different ratios: ~2.05% Ag in atomic ratio and ~8.69% Ag in weight ratio. In addition, the EDS mapping result to display the distribution of Ag and Si elements on the substrate was shown in Fig. S8.

Moreover, the SERS performance of AgNPs@Si SERS substrate was also investigated. First, the reproducibility of SERS substrate was studied by collecting the SERS spectra of 4-MBA from 100 random spots on the surface of SERS substrate. As displayed in Fig. 1D, the spectra of 4-MBA are almost identical of AgNPs@Si chip and the relative standard deviation (RSD) value of Raman intensity of 4-MBA at 1073 cm^{-1} was ~5.42%, indicating the achieved SERS substrate has a good reproducibility and uniformity of Raman signals. The robust reproducibility of the SERS-active substrate is mainly attributed to the deposition of AgNPs on the surface of silicon wafer, largely preventing them from random aggregation.

Afterward, the SERS enhancement factor (EF) of the AgNPs@Si SERS substrate was also studied. As illustrated in Fig. S1, obvious Raman signal of 4-MBA on the AgNPs@Si chip can be seen, while the intensity dispersed on the naked silicon wafer without AgNPs disposition is much weaker. The SERS EF is estimated to be ~2.1×10^6 (the detail calculation of EF is shown in the Supporting Information). This significant SERS enhancement may be attributed to the huge electromagnetic field that are produced by effectively coupled between AgNP itself and interaction AgNPs with the silicon chip [58].

3.3. Feasibility of the CHA amplification system

Two component DNA hairpins were first analyzed by the Oligo Analyzer 3.1 to forecast their conformations and other parameters (Fig. S2). The parameters are ΔH (enthalpy change), ΔG (gibbs free energy), and ΔS (entropy change) respectively. According to the Gibbs–Helmholtz (G-H) equation: $\Delta G = \Delta H - T\Delta S$, the designed hairpin structure is more stable and has rarely other secondary structure when the values of parameters are smaller, which is benefit for the CHA reaction to decrease the background signal

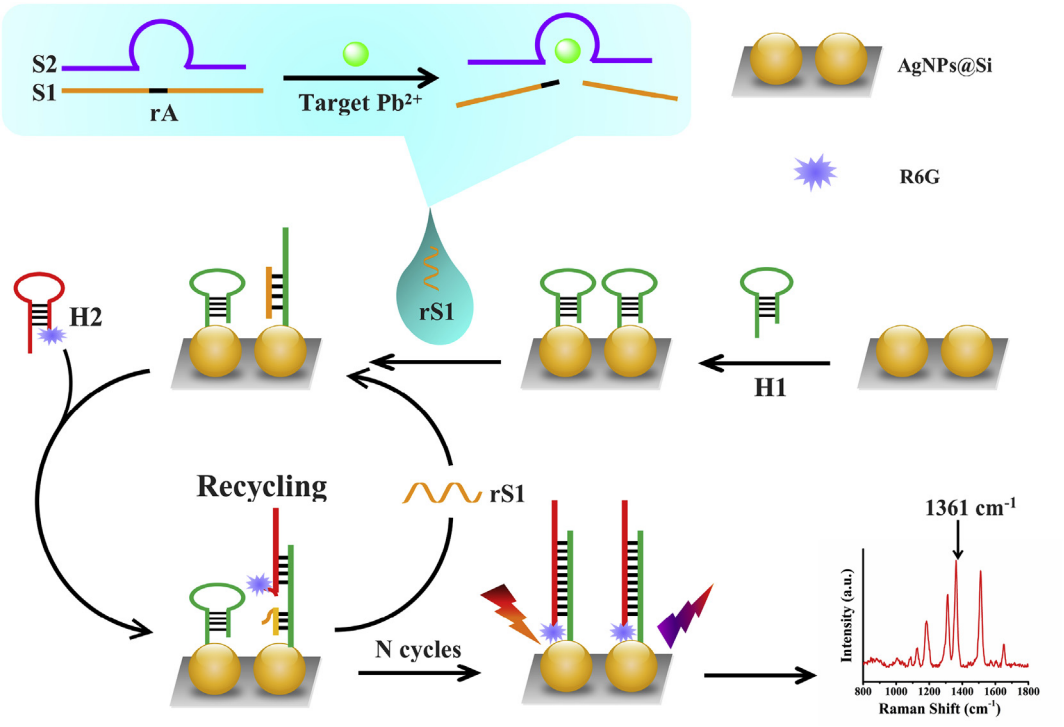

Scheme 1. Schematic illustration of CHA amplification-based SERS sensing platform for Pb^{2+} detection.

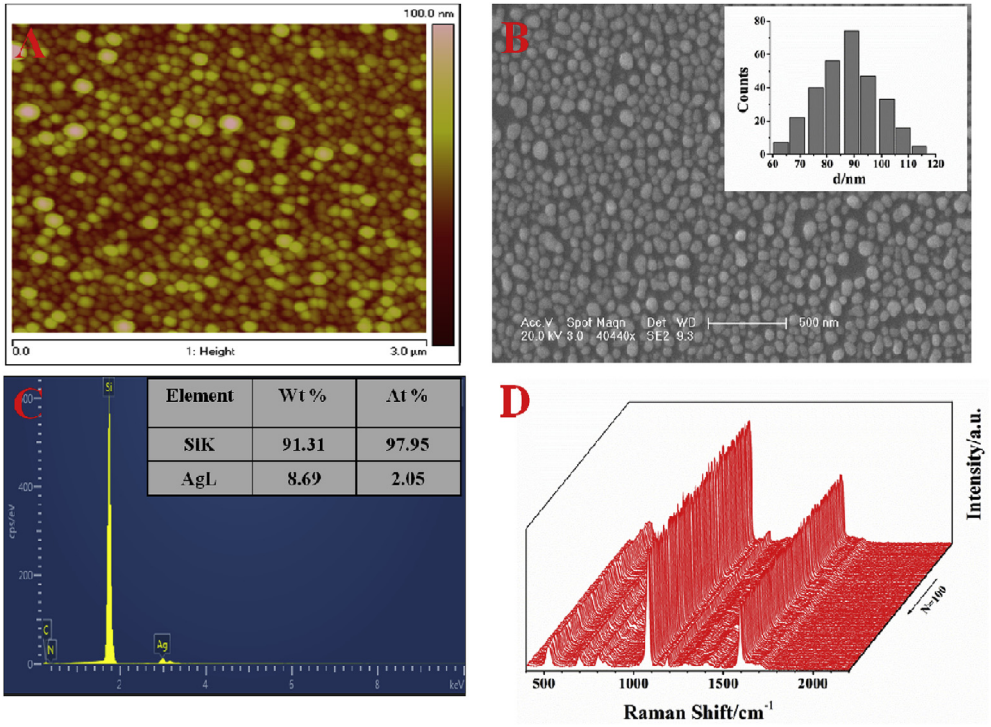

Fig. 1. (A) An AFM image of the as-prepared AgNPs@Si SERS substrate. The AFM image is obtained from an area of 5 × 5 μm^2. (B) An SEM image of the as-prepared SERS substrate. (C) The elemental ratio of AgNPs@Si chip calculated by EDX spectroscopy. (D) SERS spectra of 4-MBA from 100 random spots on the surface of AgNPs@Si substrate.

[51,59]. Based on the aforementioned principle, H1 and H2 are designed and their structures are shown in Fig. S2. As exhibited in Fig. S2, the melting temperature of H1 and H2 are 66.7 °C, and 69 °C respectively, which are much higher than the reaction temperature (37 °C).

To further testify the feasibility of the CHA reaction, the sequences and products of CHA amplification are characterized by employing 5% agarose gel. As illustrated in Fig. S3A, lane 1–8

represent DNA marker, H1, H2, DNAzymes (S1–S2), H1+H2+DNAzymes, H1+H2+Pb^{2+}, H1+H2, and H1+H2+the products of Pb^{2+} and DNAzymes respectively. In the absence of target Pb^{2+}, H1 and H2 maintain stable, indicating the cross-reaction between H1 and H2 is negligible (lane 7). Upon addition of the products of Pb^{2+} and DNAzymes, a mixture of H1 and H2 appears a new band (lane 8), suggesting that the products of Pb^{2+} and DNAzymes can trigger the CHA amplification. In addition, the feasibility of the Pb^{2+}-DNAzyme assistant CHA amplification system was further verified by Raman spectrum and the result was illustrated in Fig. S3B. These results indicate the CHA-based SERS sensing strategy for the analysis of Pb^{2+} is feasible.

3.4. Optimization of experimental conditions

The property of this developed SERS sensing platform can be potentially affected by the concentration ratio between H1 and H2, the pH value of reaction system, the CHA incubating time, and the reaction time with Pb^{2+}. Different analytical conditions were optimized in this work. First of all, the concentration ratio between H1 and H2 is investigated. As shown in Fig. S4, as the concentration ratio between H1 and H2 increases (from 1:4 to 1:1), the value of normalized Raman intensity ($I_{\text{with Pb2+}}/I_{BG}$) first increases and then decreases (after 1:1). This is because increasing concentration ratio between H1 and H2 can lead to the production more H1–H2 complexes upon CHA amplification. However, a higher concentration ratio between H1 and H2 can result in an inadequate hybridization between H1 and H2, and thus decreased signal responses are observed. These results indicate that the optimum concentration ratio between H1 and H2 is 1:1. Second, the pH value of reaction system is an important factor to the Pb^{2+} cleavage reaction, and the activity of DNAzyme is largely affected by the pH value [60]. Therefore, the effect of pH on the sensing platform is further studied. As illustrated in Fig. S5, the normalized Raman intensity increases with the increase of pH value and achieves maximum at pH 7.4 while it decreases with the further increasing pH, indicating the optimum pH value of sensing system is 7.4. Owing to Pb^{2+} has already precipitated at high pH value, therefore, it is unnecessary to obtain a meaningful value at high pH. The signal amplification of the sensing platform and the detection of the target are highly affected by the CHA incubating time. Therefore, the influence of CHA incubating time is also investigated in Fig. S6. As the increase of incubating time, the normalized Raman intensity ascends. When the incubating time exceeds to 60 min, the value of normalized Raman intensity reaches maximum value. Hence, 60 min is the optimal incubating time for CHA amplification. Furthermore, the cleavage time of Pb^{2+} is a significant factor in this experiment. The cleavage time between substrate oligonucleotide and Pb^{2+} directly influent the efficiency and the detecting result. In this work, experiments were conducted with different Pb^{2+} cleavage time ranging from 10 to 60 min for optimization of the Pb^{2+} cleavage time. Experimental date is exhibited in Fig. S7 and the result indicates that the normalized Raman intensity obtains a peak value at 30 min, suggesting that 30 min is the optimum Pb^{2+} cleavage time.

3.5. Determination of target Pb^{2+}

Under the optimal experimental conditions, this developed enzyme-free SERS platform was employed to detect different concentrations of target Pb^{2+}. In this work, to reduce systematic errors, the normalized Raman intensity ($I_{\text{with Pb2+}}/I_{BG}$) is used. Obviously, a perfect linear relationship between $I_{\text{with Pb2+}}/I_{BG}$ and the logarithmic concentration of target Pb^{2+} is achieved and the linear range is from 1 pM to 100 nM (Fig. 2B). The corresponding regression equation is $Y = 63.25 + 5.09Log_{10}X$ ($R^2 = 0.998$). Moreover, the robust sensing strategy possesses highly sensitivity because of its relatively good SERS enhancement and the merit of CHA amplification, making the detection of target Pb^{2+} with a limit of detection (LOD) of 0.42 pM (S/N = 3) (the detail of LOD calculation method is shown in the supporting information), suggesting the excellent sensitivity for Pb^{2+} determination. A comparison with other strategies for the detection of target Pb^{2+} employing different techniques are shown in Table S2. Compared to most of other prevalent methods for Pb^{2+} detection, including colormetric [61], electrochemical [62,63], and fluorescent [64] etc., the CHA-based SERS sensing strategy proposed in our work has a comparatively lower or at least a similar detection limit. More importantly, this proposed SERS sensing platform avoids sophisticated instrument and complicated operation, providing an on-site, sensitive, and specific approach for Pb^{2+} determination with a portable Raman spectrometer.

3.6. Selectivity of the Pb^{2+} assay

To further study the specificity of the proposed strategy, many kinds of other metal ions including Cu^{2+}, Zn^{2+}, Ca^{2+}, Ni^{2+}, Co^{2+}, Ba^{2+}, Mn^{2+}, Cd^{2+}, Hg^{2+}, and Fe^{2+} were added into the sensing system, respectively. As displayed in Fig. 3, only Pb^{2+} can cause a

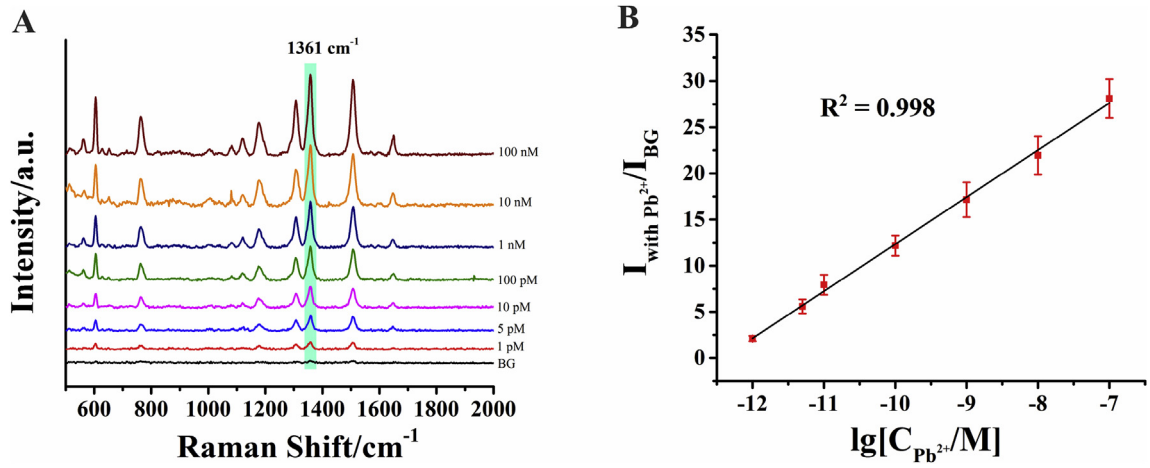

Fig. 2. (A) SERS spectra of R6G of the Pb^{2+} with different concentrations (1 pM-100 nM). Background (BG) stands for distilled water. (B) The linear fitting of Raman intensity (at 1361 cm^{-1}) with logarithmic Pb^{2+} concentrations.

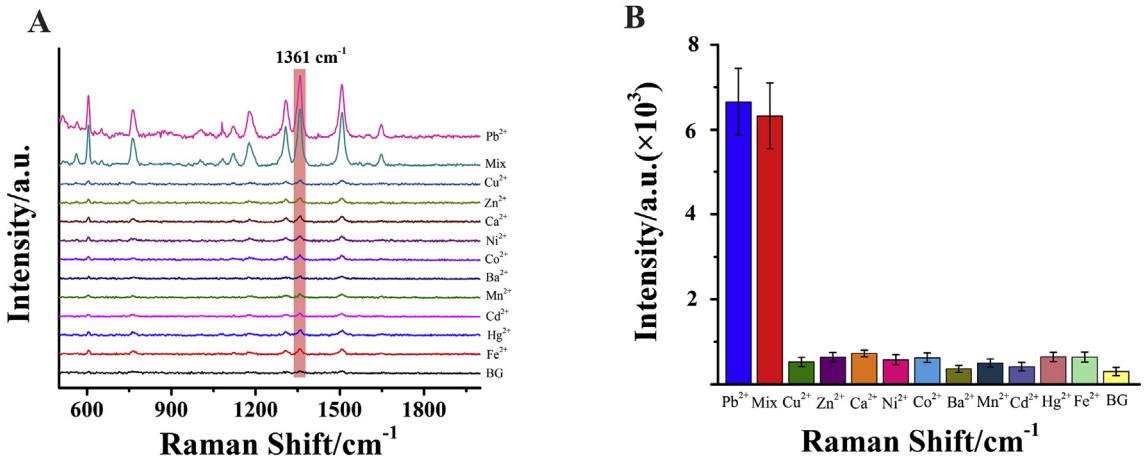

Fig. 3. (A) SERS spectra and (B) corresponding Raman intensities at 1361 cm^{-1} in the presence of various kinds of metal ions (Pb^{2+}, Cu^{2+}, Zn^{2+}, Ca^{2+}, Ni^{2+}, Co^{2+}, Ba^{2+}, Mn^{2+}, Cd^{2+}, Hg^{2+}, and Fe^{2+}, 1.0 nM for each ions) and a mixture of these metal ions. BG represents background signal. Error bar stands for the standard deviation of measurement collected from three independent experiments.

remarkable SERS increase, but other metal ions cannot cause obvious SERS response. Moreover, the SERS intensity of to Pb^{2+} in the presence of all other metal ions is almost the same as that in the presence of Pb^{2+} only. Those results demonstrate that the selectivity of the developed SERS sensing platform is excellent.

3.7. *Reproducibility*

It is well known that the reproducibility of SERS signal is highly significant for SERS sensor. Herein, the reproducibility of the developed SERS sensing strategy is investigated for the analysis of Pb^{2+} and the RSD value is estimated to be 8.73% (Fig. 4B), which is obtained by collecting from 40 random spots on the probe surface toward target Pb^{2+} with the concentration of 1.0 nM (Fig. 4A). Moreover, the reliability of the proposed SERS platform was evaluated via collection from 10 different SERS chips in the same experimental conditions (Fig. 4C). As shown in Fig. 4D, the RSD of the values of I_{1361} is 8.65%, indicating the satisfactory reproducibility of the proposed sensing strategy.

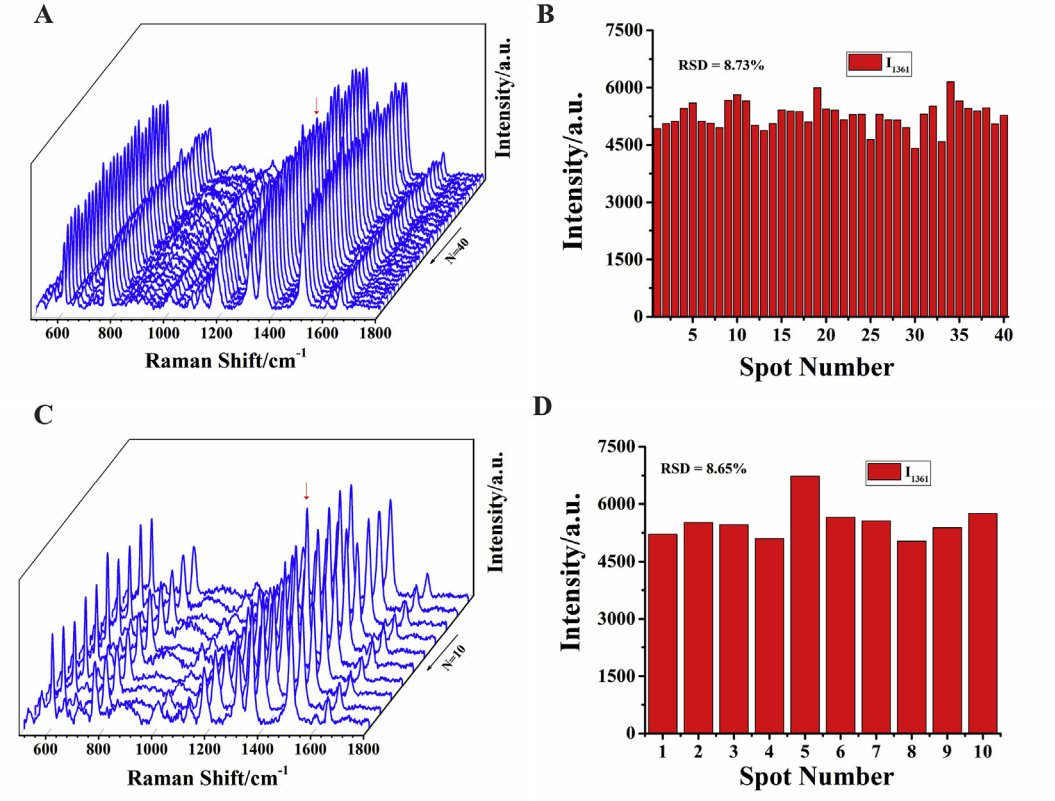

Fig. 4. (A) SERS spectra from 40 random spots on the surface of chip with the concentration of 1.0 nM target Pb^{2+} and (B) corresponding histogram for the value of I_{1361} collected from 40 different spots. (C) SERS spectra and (D) histogram for the value of I_{1361} from 10 different SERS chips.

3.8. Reusability

Besides to the sensitivity, selectivity, and reproducibility of the proposed SERS sensing platform, the reusability is also significant in its practical applications. Fortunately, the proposed SERS platform has a good reusability upon supplementation of target Pb^{2+} to forming R6G-labeled H1–H2 duplexes. As illustrated in Fig. S9a, after washing with water once, the washed SERS probe was then used to another round of determination. Fig. S9b shows three-cycles Raman spectra of the CHA-based SERS strategy in the determination of 1.0 nM Pb^{2+}. During each cycle, the Raman intensity of R6G at 1361 cm^{-1} sharply decreased when washed with water, while its intensity readily recovered almost to the initial state after addition of the Pb^{2+}-assisted CHA product. The RSD value of the developed SERS signals is 8.1% within three cycles (Fig. S9c), demonstrating the good reusability of the proposed sensing strategy.

3.9. Application in real samples

To demonstrate the practical application of the developed strategy, it was applied to detect the spiked with different Pb^{2+} concentrations in real environment water samples, which were obtained from Wujiang River (Chongqing, China). These samples were analyzed by employing our developed sensing platform and the ICP-MS, respectively. As shown in Table S3, these data achieved by the developed method indicate a good agreement with these detected by ICP-MS. This result indicates the proposed sensing strategy can be applied for Pb^{2+} determination in real environment water samples with good reliability and accuracy.

4. Conclusions

In this system, a robust SERS sensing platform has been developed for highly sensitive and specific analysis of target Pb^{2+} based on a Pb^{2+}-DNAzyme assistant CHA amplification. This proposed method combined the high specificity of Pb^{2+}-based DNAzymes with the signal amplification of CHA reaction, which achieved the excellent performance for highly sensitive and specific determination of Pb^{2+}. Taking advantages of the Pb^{2+}-specific DNAzymes and CHA signal amplification, a LOD of 0.42 pM for target Pb^{2+} has been obtained with a wide linear range and a good selectivity is also achieved. Moreover, this proposed sensing method for Pb^{2+} determination can be applicable to the real environment system and the recovery was satisfactory.

CRediT authorship contribution statement

Yan Wu: Methodology, Conceptualization, Software, Visualization, Validation, Writing - original draft, Writing - review & editing, Supervision, Funding acquisition, Project administration. **Cuicui Fu:** Methodology, Conceptualization, Formal analysis, Writing - original draft, Funding acquisition, Project administration. **Jie Xiang:** Formal analysis, Writing - original draft. **Yulian Cao:** Conceptualization, Software, Visualization. **Yu Deng:** Conceptualization, Writing - original draft, Investigation, Validation. **Rui Xu:** Validation, Methodology, Conceptualization. **Huan Zhang:** Methodology, Visualization, Validation, Writing - original draft. **Wenbing Shi:** Supervision, Writing - review & editing, Funding acquisition, Project administration.

Declaration of competing interest

The authors declare that they have no known competing financial interests or personal relationships that could have appeared to influence the work reported in this paper.

Acknowledgements

This research was financially supported by the National Natural Science Foundation of China (No. 21804011 and No. 21705009), the Basic Research Project of Science and Technology Commission of Chongqing (No. cstc2018jcyjAX0721), the Municipal Education Commission of Chongqing (No. KJQN201801404).

Appendix A. Supplementary data

Supplementary data to this article can be found online at https://doi.org/10.1016/j.aca.2020.06.038.

References

[1] B.B. Rodriguez, J.A. Bolbot, I.E. Tothill, Development of urease and glutamic dehydrogenase amperometric assay for heavy metals screening in polluted samples, Biosens. Bioelectron. 19 (2004) 1157–1167.
[2] H. Needleman, Lead poisoning, Annu. Rev. Med. 55 (2004) 209–222.
[3] S. Panich, K.A. Wilson, P. Nuttall, C.K. Wood, T. Albrecht, J.B. Edel, Label-free Pb (II) whispering gallery mode sensing using self-assembled glutathione-modified gold nanoparticles on an optical microcavity, Anal. Chem. 86 (2014) 6299–6306.
[4] Y. Huang, Y. Ma, Y. Chen, X. Wu, L. Fang, Z. Zhu, C.J. Yang, Target-responsive DNAzyme cross-linked hydrogel for visual quantitative detection of lead, Anal. Chem. 86 (2014) 11434–11439.
[5] M. Ghaedi, F. Ahmadi, A. Shokrollahi, Simultaneous preconcentration and determination of copper, nickel, cobalt and lead ions content by flame atomic absorption spectrometry, J. Hazard Mater. 142 (2007) 272–278.
[6] A.C. Davis, C.P. Calloway Jr., B.T. Jones, Direct determination of cadmium in urine by tungsten-coil inductively coupled plasma atomic emission spectrometry using palladium as a permanent modifier, Talanta 71 (2007) 1144–1149.
[7] Y. Izumi, F. Kiyotaki, T. Minato, Y. Seida, X-ray absorption fine structure combined with fluorescence spectrometry for monitoring trace amounts of lead adsorption in the environmental conditions, Anal. Chem. 74 (2002) 3819–3823.
[8] E.P. Oliveira, L. Yang, R.E. Sturgeon, R.E. Santelli, M.A. Bezerra, S.N. Willie, R. Capilla, Determination of trace metals in high-salinity petroleum produced formation water by inductively coupled plasma mass spectrometry following on-line analyte separation/preconcentration, J. Anal. At. Spectrom. 26 (2011) 578–585.
[9] T. Li, E. Wang, S. Dong, Lead (II)-induced allosteric G-quadruplex DNAzyme as a colorimetric and chemiluminescence sensor for highly sensitive and selective Pb^{2+} detection, Anal. Chem. 82 (2010) 1515–1520.
[10] W. Yun, D. Cai, J. Jiang, P. Zhao, Y. Huang, G. Sang, Enzyme-free and label-free ultra-sensitive colorimetric detection of Pb^{2+} using molecular beacon and DNAzyme based amplification strategy, Biosens. Bioelectron. 80 (2016) 187–193.
[11] Z. Huang, J. Chen, Z. Luo, X. Wang, Y. Duan, Label-free and enzyme-free colorimetric detection of Pb^{2+} based on RNA cleavage and annealing-accelerated hybridization chain reaction, Anal. Chem. 91 (2019) 4806–4813.
[12] Y. Yu, Y. Hong, P. Gao, M.K. Nazeeruddin, Glutathione modified gold nanoparticles for sensitive colorimetric detection of Pb^{2+} ions in rainwater polluted by leaking perovskite solar cells, Anal. Chem. 88 (2016) 12316–12322.
[13] X. Yang, J. Xu, X. Tang, H. Liu, D. Tian, A novel electrochemical DNAzyme sensor for the amplified detection of Pb^{2+} ions, Chem. Commun. 46 (2010) 3107–3109.
[14] S. Tang, P. Tong, H. Li, J. Tang, L. Zhang, Ultrasensitive electrochemical detection of Pb^{2+} based on rolling circle amplification and quantum dots tagging, Biosens. Bioelectron. 42 (2013) 608–611.
[15] M. Li, Z. Li, C. Liu, Y. Chang, J. Wen, H. Zhao, H. Cao, Y. Zhang, D. Liu, Amino-modification and successive electrochemical reduction of graphene oxide for highly sensitive electrochemical detection of trace Pb^{2+}, Carbon 109 (2016) 479–486.
[16] J.-H. Hwang, M.A. Islam, H. Choi, T.-J. Ko, K.L. Rodriguez, H.-S. Chung, Y. Jung, W.H. Lee, Improving electrochemical Pb^{2+} detection using a vertically aligned 2D MoS_2 nanofilm, Anal. Chem. 91 (2019) 11770–11777.
[17] X.-H. Zhao, R.-M. Kong, X.-B. Zhang, H.-M. Meng, W.-N. Liu, W. Tan, G.-L. Shen, R.-Q. Yu, Graphene–DNAzyme based biosensor for amplified fluorescence "turn-on" detection of Pb^{2+} with a high selectivity, Anal. Chem. 83 (2011) 5062–5066.
[18] X. Niu, Y. Zhong, R. Chen, F. Wang, Y. Liu, D. Luo, A "turn-on" fluorescence sensor for Pb^{2+} detection based on graphene quantum dots and gold nanoparticles, Sensor. Actuator. B Chem. 255 (2018) 1577–1581.
[19] T. Li, S. Dong, E. Wang, A lead (II)-driven DNA molecular device for turn-on fluorescence detection of lead (II) ion with high selectivity and sensitivity,

J. Am. Chem. Soc. 132 (2010) 13156–13157.
[20] J. Wang, Z. Zhang, X. Gao, X. Lin, Y. Liu, S. Wang, A single fluorophore ratiometric nanosensor based on dual-emission DNA-templated silver nanoclusters for ultrasensitive and selective Pb^{2+} detection, Sensor. Actuator. B Chem. 282 (2019) 712–718.
[21] Y. Wang, J. Irudayaraj, A SERS DNAzyme biosensor for lead ion detection, Chem. Commun. 47 (2011) 4394–4396.
[22] Y. Shi, H. Wang, X. Jiang, B. Sun, B. Song, Y. Su, Y. He, Ultrasensitive, specific, recyclable, and reproducible detection of lead ions in real systems through a polyadenine-assisted, surface-enhanced Raman scattering silicon chip, Anal. Chem. 88 (2016) 3723–3729.
[23] Y.W. Fen, W.M.M. Yunus, N.A. Yusof, Surface plasmon resonance optical sensor for detection of Pb^{2+} based on immobilized p-tert-butylcalix [4] arene-tetrakis in chitosan thin film as an active layer, Sensor. Actuator. B Chem. 171 (2012) 287–293.
[24] Y. Peng, Y. Li, L. Li, J.-J. Zhu, A label-free aptasensor for ultrasensitive Pb^{2+} detection based on electrochemiluminescence resonance energy transfer between carbon nitride nanofibers and Ru $(phen)_3^{2+}$, J. Hazard Mater. 359 (2018) 121–128.
[25] H.-M. Deng, L.-J. Huang, Y.-Q. Chai, R. Yuan, Y.-L. Yuan, Ultrasensitive photoelectrochemical detection of multiple metal ions based on wavelength-resolved dual-signal output triggered by click reaction, Anal. Chem. 91 (2019) 2861–2868.
[26] R.R. Breaker, G.F. Joyce, A DNA enzyme that cleaves RNA, Chem. Biol. 1 (1994) 223–229.
[27] L.-J. Xu, Z.-C. Lei, J. Li, C. Zong, C.J. Yang, B. Ren, Label-free surface-enhanced Raman spectroscopy detection of DNA with single-base sensitivity, J. Am. Chem. Soc. 137 (2015) 5149–5154.
[28] B. Sharma, P. Bugga, L.R. Madison, A.-I. Henry, M.G. Blaber, N.G. Greeneltch, N. Chiang, M. Mrksich, G.C. Schatz, R.P. Van Duyne, Bisboronic acids for selective, physiologically relevant direct glucose sensing with surface-enhanced Raman spectroscopy, J. Am. Chem. Soc. 138 (2016) 13952–13959.
[29] D. Zhang, H. You, L. Yuan, R. Hao, T. Li, J. Fang, Hydrophobic slippery surface-based surface-enhanced Raman spectroscopy platform for ultrasensitive detection in food safety applications, Anal. Chem. 91 (2019) 4687–4695.
[30] S. He, Y.M.E. Kyaw, E.K.M. Tan, L. Bekale, M.W.C. Kang, S.S.-Y. Kim, I. Tan, K.-P. Lam, J.C.Y. Kah, Quantitative and label-free detection of protein kinase a activity based on surface-enhanced Raman spectroscopy with gold nanostars, Anal. Chem. 90 (2018) 6071–6080.
[31] C. Fu, W. Xu, H. Wang, H. Ding, L. Liang, M. Cong, S. Xu, DNAzyme-based plasmonic nanomachine for ultrasensitive selective surface-enhanced Raman scattering detection of lead ions via a particle-on-a-film hot spot construction, Anal. Chem. 86 (2014) 11494–11497.
[32] Y. Peng, L. Li, X. Yi, L. Guo, Label-free picomolar detection of Pb^{2+} using atypical icosahedra gold nanoparticles and rolling circle amplification, Biosens. Bioelectron. 59 (2014) 314–320.
[33] X. Xie, Y. Chai, Y. Yuan, R. Yuan, Dual triggers induced disassembly of DNA polymer decorated silver nanoparticle for ultrasensitive electrochemical Pb^{2+} detection, Anal. Chim. Acta 1034 (2018) 56–62.
[34] J. Zhuang, L. Fu, M. Xu, Q. Zhou, G. Chen, D. Tang, DNAzyme-based magneto-controlled electronic switch for picomolar detection of lead (II) coupling with DNA-based hybridization chain reaction, Biosens. Bioelectron. 45 (2013) 52–57.
[35] S. Tang, W. Lu, F. Gu, P. Tong, Z. Yan, L. Zhang, A novel electrochemical sensor for lead ion based on cascade DNA and quantum dots amplification, Electrochim. Acta 134 (2014) 1–7.
[36] W. Li, Y. Yang, J. Chen, Q. Zhang, Y. Wang, F. Wang, C. Yu, Detection of lead (II) ions with a DNAzyme and isothermal strand displacement signal amplification, Biosens. Bioelectron. 53 (2014) 245–249.
[37] Y. Jiang, B. Li, J.N. Milligan, S. Bhadra, A.D. Ellington, Real-time detection of isothermal amplification reactions with thermostable catalytic hairpin assembly, J. Am. Chem. Soc. 135 (2013) 7430–7433.
[38] B. Li, Y. Jiang, X. Chen, A.D. Ellington, Probing spatial organization of DNA strands using enzyme-free hairpin assembly circuits, J. Am. Chem. Soc. 134 (2012) 13918–13921.
[39] Z. Wu, H. Fan, N.S.R. Satyavolu, W. Wang, R. Lake, J.H. Jiang, Y. Lu, Imaging endogenous metal ions in living cells using a DNAzyme–catalytic hairpin assembly probe, Angew. Chem. Int. Ed. 56 (2017) 8721–8725.
[40] J. Liu, P. Du, J. Zhang, H. Shen, J. Lei, Sensitive detection of intracellular microRNA based on a flowerlike vector with catalytic hairpin assembly, Chem. Commun. 54 (2018) 2550–2553.
[41] Y. Zang, J. Lei, P. Ling, H. Ju, Catalytic hairpin assembly-programmed porphyrin–DNA complex as photoelectrochemical initiator for DNA biosensing, Anal. Chem. 87 (2015) 5430–5436.
[42] Y. Chu, A.-P. Deng, W. Wang, J.-J. Zhu, Concatenated catalytic hairpin assembly/hyperbranched hybridization chain reaction based enzyme-free signal amplification for the sensitive photoelectrochemical detection of human telomerase RNA, Anal. Chem. 91 (2019) 3619–3627.
[43] Y. Zhang, Y. Yan, W. Chen, W. Cheng, S. Li, X. Ding, D. Li, H. Wang, H. Ju, S. Ding, A simple electrochemical biosensor for highly sensitive and specific detection of microRNA based on mismatched catalytic hairpin assembly, Biosens. Bioelectron. 68 (2015) 343–349.
[44] Y.-X. Chen, X. Wu, K.-J. Huang, A sandwich-type electrochemical biosensing platform for microRNA-21 detection using carbon sphere-MoS_2 and catalyzed hairpin assembly for signal amplification, Sensor. Actuator. B Chem. 270 (2018) 179–186.
[45] H. Cheng, W. Li, S. Duan, J. Peng, J. Liu, W. Ma, H. Wang, X. He, K. Wang, Mesoporous silica containers and programmed catalytic hairpin assembly/hybridization chain reaction based electrochemical sensing platform for miRNA ultrasensitive detection with low background, Anal. Chem. 91 (2019) 10672–10678.
[46] Y. Liu, T. Shen, J. Li, H. Gong, C. Chen, X. Chen, C. Cai, Ratiometric fluorescence sensor for the microRNA determination by catalyzed hairpin assembly, ACS Sens. 2 (2017) 1430–1434.
[47] Y. Qin, D. Li, R. Yuan, Y. Xiang, Silver ion-stabilized DNA triplexes for completely enzyme-free and sensitive fluorescence detection of transcription factors via catalytic hairpin assembly amplification, J. Mater. Chem. B 7 (2019) 763–767.
[48] C. Chen, N. Li, J. Lan, X. Ji, Z. He, A label-free colorimetric platform for DNA via target-catalyzed hairpin assembly and the peroxidase-like catalytic of graphene/Au-NPs hybrids, Anal. Chim. Acta 902 (2016) 154–159.
[49] C. Park, H. Park, H.J. Lee, H.S. Lee, K.H. Park, C.-H. Choi, S. Na, Double amplified colorimetric detection of DNA using gold nanoparticles, enzymes and a catalytic hairpin assembly, Microchim. Acta 186 (2019) 34.
[50] X. Li, W. Cheng, D. Li, J. Wu, X. Ding, Q. Cheng, S. Ding, A novel surface plasmon resonance biosensor for enzyme-free and highly sensitive detection of microRNA based on multi component nucleic acid enzyme (MNAzyme)-mediated catalyzed hairpin assembly, Biosens. Bioelectron. 80 (2016) 98–104.
[51] J. Li, P. Lei, S. Ding, Y. Zhang, J. Yang, Q. Cheng, Y. Yan, An enzyme-free surface plasmon resonance biosensor for real-time detecting microRNA based on allosteric effect of mismatched catalytic hairpin assembly, Biosens. Bioelectron. 77 (2016) 435–441.
[52] F. Qi, Y. Han, Z. Ye, H. Liu, L. Wei, L. Xiao, Color-coded single-particle pyrophosphate assay with dark-field optical microscopy, Anal. Chem. 90 (2018) 11146–11153.
[53] S. Wang, Z. Ye, X. Wang, L. Xiao, Etching of single-MnO_2-coated gold nanoparticles for the colorimetric detection of organophosphorus pesticides, ACS Appl. Nano Mater. 2 (2019) 6646–6654.
[54] Z. Ye, R. Weng, Y. Ma, F. Wang, H. Liu, L. Wei, L. Xiao, Label-free, single-particle, colorimetric detection of permanganate by GNPs@Ag core–shell nanoparticles with dark-field optical microscopy, Anal. Chem. 90 (2018) 13044–13050.
[55] N. Chen, P. Ding, Y. Shi, T. Jin, Y. Su, H. Wang, Y. He, Portable and reliable surface-enhanced Raman scattering silicon chip for signal-on detection of trace trinitrotoluene explosive in real systems, Anal. Chem. 89 (2017) 5072–5078.
[56] H. Wang, X. Jiang, Y. He, Highly sensitive and reproducible silicon-based surface-enhanced Raman scattering sensors for real applications, Analyst 141 (2016) 5010–5019.
[57] H. Wang, X. Jiang, X. Wang, X. Wei, Y. Zhu, B. Sun, Y. Su, S. He, Y. He, Hairpin DNA-assisted silicon/silver-based surface-enhanced Raman scattering sensing platform for ultrahighly sensitive and specific discrimination of deafness mutations in a real system, Anal. Chem. 86 (2014) 7368–7376.
[58] Z. Peng, H. Hu, M.I.B. Utama, L.M. Wong, K. Ghosh, R. Chen, S. Wang, Z. Shen, Q. Xiong, Heteroepitaxial decoration of Ag nanoparticles on Si nanowires: a case study on Raman scattering and mapping, Nano Lett. 10 (2010) 3940–3947.
[59] K. Datta, V.J. LiCata, Thermodynamics of the binding of Thermus aquaticus DNA polymerase to primed-template DNA, Nucleic Acids Res. 31 (2003) 5590–5597.
[60] Z. Wang, J.H. Lee, Y. Lu, Label-free colorimetric detection of lead ions with a nanomolar detection limit and tunable dynamic range by using gold nanoparticles and DNAzyme, Adv. Mater. 20 (2008) 3263–3267.
[61] H. Wang, L. Yang, S. Chu, B. Liu, Q. Zhang, L. Zou, S. Yu, C. Jiang, Semi-quantitative visual detection of lead ions with a smartphone via a colorimetric paper-based analytical device, Anal. Chem. 91 (2019) 9292–9299.
[62] L. Cui, J. Wu, J. Li, H. Ju, Electrochemical sensor for lead cation sensitized with a DNA functionalized porphyrinic metal-organic framework, Anal. Chem. 87 (2015) 10635–10641.
[63] X. Wang, C. Yang, S. Zhu, M. Yan, S. Ge, J. Yu, 3D origami electrochemical device for sensitive Pb^{2+} testing based on DNA functionalized iron-porphyrinic metal-organic framework, Biosens. Bioelectron. 87 (2017) 108–115.
[64] D. Peng, Y. Li, Z. Huang, R.-P. Liang, J.-D. Qiu, J. Liu, Efficient DNA-catalyzed porphyrin metalation for fluorescent ratiometric Pb^{2+} detection, Anal. Chem. 91 (2019) 11403–11408.